Iranian Journal of Electrical and Electronic Engineering

Journal Homepage: ijeee.iust.ac.ir

[DOI: 10.22068/IJEEE.14.1.49]

Downloaded from ijeee.iust.ac.ir at 11:41 IRDT on Saturday September 5th 2020

Hybrid Z-Source DC-DC Converter with ZVZCS and Power Transformer Resetting: Design, Modeling, and Fabrication

H. Torkaman*(C.A.) and T. Hemmati*

Abstract: This paper introduces a novel two transistors forward topology employing a z-source to achieve ZVZCS and power transformer resetting for various applications. Comparing with the forward converter, this topology has the advantage of displaying ZCS condition with an added Z-Source and no additional switches when the switches turn on, and that ZVS condition happens when the switches turn off. Duty cycle of the topology can exceed 50 percent. As a result, these converters are suitable for applications with high efficiency. In this paper, structure and properties of the topology will be discussed in details. Then the design principles will be presented. Finally, the benefits aforementioned will be approved in practice through a simple forward converter.

Keywords: Zero Voltage Switching (ZVS), Zero Current Switching (ZCS), Z-Source Converters, Forward DC-DC Converter.

1 Introduction

FORWARD converters are known as low-power devices throughout the industry [1,2]. With the creation of the resonant transformer core reset, duty cycle may increase to higher than 50 percent and this has led to various applications of the forward converters [3-6]. Comparing the single-transistor forward converter, the two transistor forward converter has wider range of applications due to the low stress of the switches [7,8]. This is the first advantage of two-transistor forward converter. To reduce the stress of the switches in two transistors forward converter, some methods in [9-11] are suggested.

In forward converter, the transformer leakage inductance makes a great impact when the switches are shut down. Therefore, protective auxiliary circuits are needed in practical implementation. Resistors, capacitors and diodes can reduce switching losses and store the impulse voltages. But protective losses will reduce the efficiency. For reducing the switching losses and store impulse voltages, active protective auxiliary circuits are used [12,13]. Active protective and auxiliary circuits, lead to higher complexity and cost of the converter.

A topology in [13] has been suggested in which the ZCS condition is created for the main switch and the auxiliary switch has increased the efficiency of the converter. The topology presented in [12] has created the ZVS conditions for main switches and auxiliary switches so that the efficiency has increased. It is also possible to increase the duty cycle to exceed 50 percent.

The Z-source converter employs a unique impedance network (or circuit) to couple the converter main circuit to the power source, thus providing unique features that cannot be obtained in the traditional voltage-source (or voltage-fed) and current-source (or current-fed) converters [14,15]. Now days, the technical knowledge of the Z-sources has changed significantly. As an example, Peng has introduced some circuits of Z-sources in [16] and has brought the corresponding control solutions in [17]. The Γ-Z-source has modeled and controlled in [18,19]. The Z-sources applications have been extended through out the different bases including fuel cells [20-22], motor drives [23], power distribution systems [24-27], photovoltaic systems [28] and electrical vehicles [29].

This paper presents a new topology named novel two transistors forward topology. It employs a z-source to achieve ZVZCS and power transformer resetting that

Iranian Journal of Electrical & Electronic Engineering, 2018.
Paper first received 25 September 2017 and accepted 23 February 2018.
* The authors are with the Faculty of Electrical Engineering, Shahid Beheshti University, A.C., Tehran, Iran. 1658953571.
E-mails: H_Torkaman@sbu.ac.ir and hemati@sbu.ac.ir.
Corresponding Author: H. Torkaman.

www.SID.ir

Archive of SID

[DOI: 10.22068/IJEEE.14.1.49]

Downloaded from ijeee.iust.ac.ir at 11:41 IRDT on Saturday September 5th 2020

creates ZCS and ZVS conditions when respectively, the switches are turned on and off. By making ZVZCS condition, a higher efficiency is created. It is also possible to increase the duty cycle to more than 50 percent. In this regard, in Section 2 the new structure will be described with different working range of the converter. The design considerations will be presented in Section 3 and converter characteristics are achieved compared to conventional converters. The practical features of the converter are discussed in the Section 4. Finally, a summary of the salient results is presented in Section 5.

2 Operation Principle

The circuit of the combined two transistors forward converter and Z-source is shown in Fig. 1. C_1 and C_2 are capacitors and L_1 and L_2 are inductors of the impedance source. Diode D_1 prevents the return of the power to the input source. Capacitors C_3 and C_4 are respectively parallel to diodes D_2 and D_3 which have been placed so as to create better conditions for ZVS and transformer core reset. Switches S_1 and S_2 are converter switches. Inductor L_m is transformer magnetizing inductance and L_S is leakage inductance. To analyze the converter, the steady-state operating conditions are pre-assumed. Since the output capacitor has a high capacity, the output voltage is constant. The converter overall performance is divided into six intervals. The current and the voltage waveforms of circuit elements are illustrated in Fig. 2 and Fig. 3. The behavior of the converter is shown in Fig. 4 in separate working intervals.

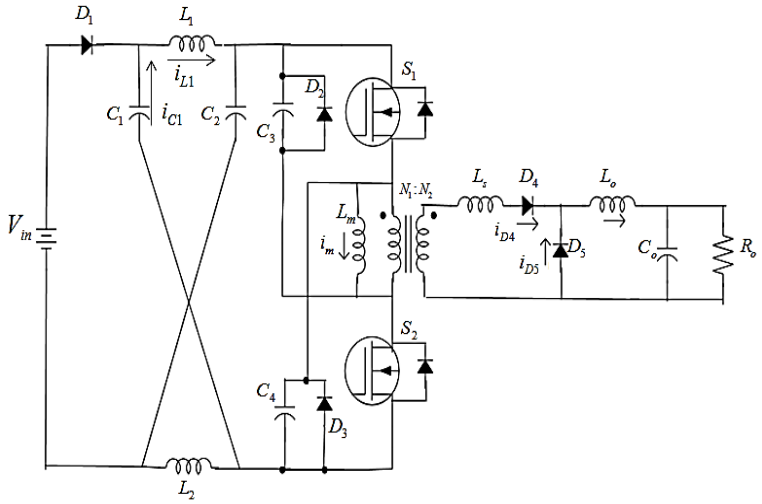


Fig. 1 Novel Z-Source two transistors forward ZVZCS, DC-DC converter.

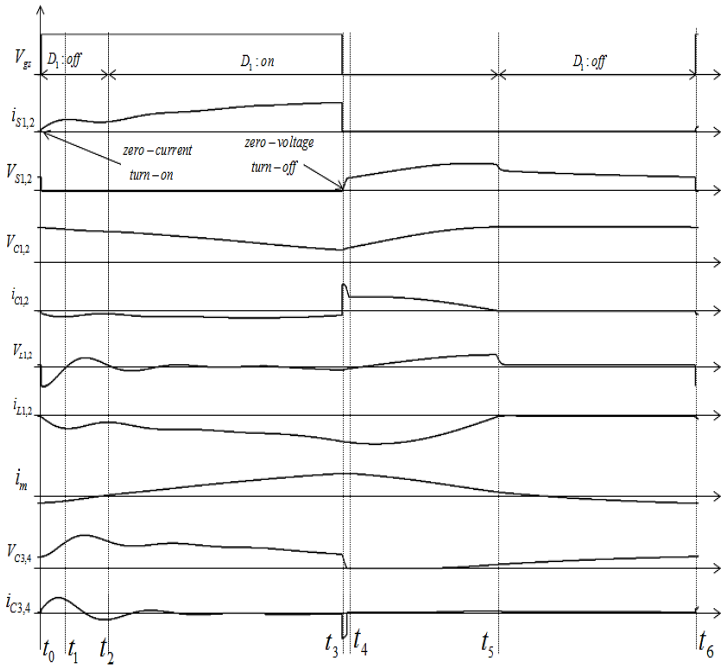


Fig. 2 Waveforms of the proposed converter.

www.SID.ir

Archive of SID

[DOI: 10.22068/IJEEE.14.1.49]

Downloaded from ijeee.iust.ac.ir at 11:41 IRDT on Saturday September 5th 2020

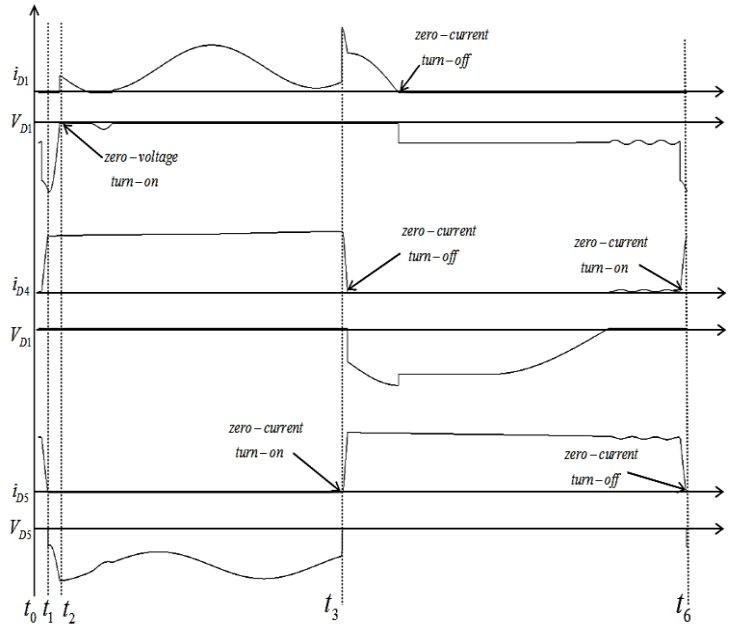


Fig. 3 The diodes waveforms of the proposed converter.

Stage 2 [t_1, t_2]: As it is shown in Fig. 2, Fig. 3 and Fig. 4(b). The energy of the inductors L_1, L_2 and of the capacitors C_1 and C_2 are being transferred to the load. Part of their energy is spent charging capacitors C_3 and C_4 which are selected in much smaller capacities when compared to the source impedance capacitors. Capacitors C_3 and C_4 are fully charged in this stage and then begin to transfer their energy to the load through the transformer. Rectifier diode D_4 is conducting the current. Free-wheeling D_5 is in the reverse bias. This state is different from the previous step because in this stage, Inductors L_1, L_2 are discharging. At the end of this stage source impedance inductors are discharged while the capacitors are still being charged.

Stage 3 [t_2, t_3]: As it is shown in Fig. 2, Fig. 3 and Fig.4(c) inductors L_1 and L_2 are charged, in addition, the capacitors C_1 and C_2 are discharged. The capacitors C_3 and C_4 are discharging. As a result, the gradient current of the switches S_1 and S_2 increases. Rectifier diode D_4 is conducting the current. Free-wheeling D_5 is in the reverse bias. At the end of this stage, inductors L_1 and L_2 are charging. The energy of the capacitors C_1, C_2, C_3 and C_4 is in the minimum value over the entire period.

Stage 4 [t_3, t_4]: As it is shown in Fig. 2, Fig. 3 and Fig. 4(d). The energy of the capacitors C_3 and C_4 which is already reached the minimum value in stage 3, sharply arrived to zero at the moment of the switches' turn off S_1 and S_2 and its energy is transferred to the source impedance. The voltage of the switches becomes zero in the moment of turn off of the Switches and the switches are turned off under ZVS conditions. The selection of the capacitors C_3 and C_4 is of importance in creating ZVS conditions and they should be smaller than the capacitors C_1 and C_2 to either transfer their energy completely and do not create a strong current. If their value is smaller than a specific amount, ZVS condition does not happen and if their value is higher, a strong current is created which leads to a damage to the switches. Capacitors C_3 and C_4 charge the capacitors C_1 and C_2 while inductors L_1 and L_2 are also being charged. In this stage the freewheeling diode D_5 is turned on and rectifier diode D_4 is turned off.

Stage 5 [t_4, t_5]: As it is shown in Fig. 2, Fig. 3, Fig. 4(e), transformer magnetizing inductance and inductors L_1 and L_2 are discharging. The freewheeling diodes D_2 and D_3 start conducting current in the beginning of the stage. Capacitors C_1, C_2, C_3 and C_4 are charging. The freewheeling diode D_5 conducts the current of L_o to the load and rectifier diode D_4 is turned off. Impedance source inductors have been fully discharged at the end of this phase and also impedance source capacitors have been fully charged in the end of this stage.

Stage 6 [t_5, t_6]: As it is shown in Fig. 2, Fig. 3 and Fig. 4(f), inductors L_1 and L_2 are discharged and capacitors C_1 and C_2 are fully charged. Freewheeling diodes D_2 and D_3 are in reverse bias because the current of the transformer magnetic inductance is zero. Since the capacitors C_3 and C_4 are fully discharged, they start to charge by source impedance. Subsequently, the charging current passes through the transformer in the reverse direction of the transformer magnetizing current. At this moment, Transformer magnetizing current will become negative and the transformer core will reset. The freewheeling diode D_5 conducts the current of L_o to the load and rectifier diode D_4 is turned off.

www.SID.ir

Archive of SID

[DOI: 10.22068/IJEEE.14.1.49]

Downloaded from ijeee.iust.ac.ir at 11:41 IRDT on Saturday September 5th 2020

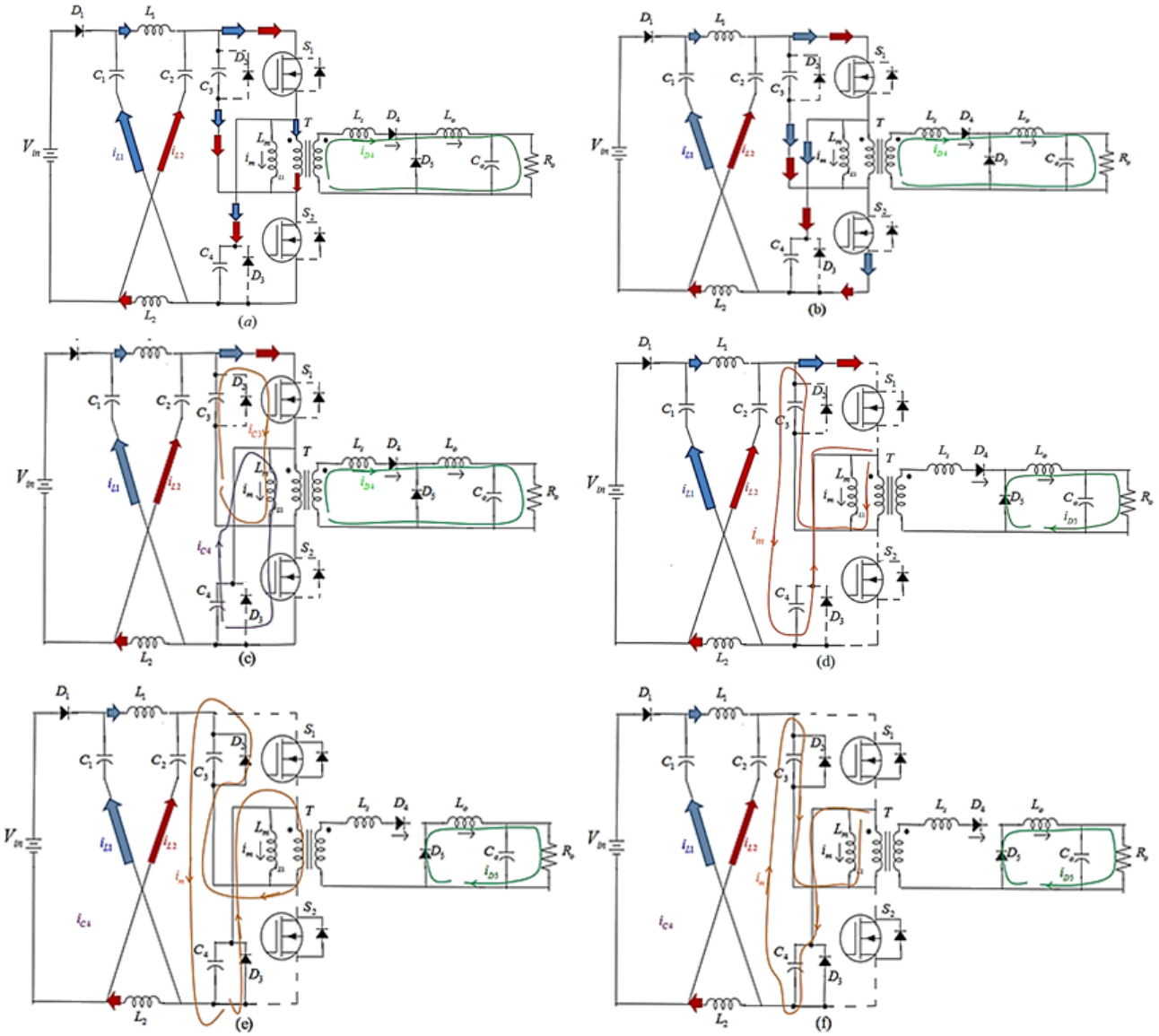


Fig. 4 The equivalent circuit of each stage: a) Stage 1 [t_0, t_1], b) Stage 2 [t_1, t_2], c) Stage 3 [t_2, t_3], d) Stage 4 [t_3, t_4], e) Stage 5 [t_4, t_5], and f) Stage 6 [t_5, t_6].

3 Design Consideration

In order to reset the transformer core, the maximum duty cycle will be 50 percent in the forward converters. For increasing duty cycle to over 50%, the effective voltage of the transformer should be increased when the switches are turned off. To reduce the switching losses, soft switching is needed. To achieve these goals, the two transistor forward converter will be combined with a source-impedance that is shown in Fig. 1.

3.1 ZCS at the Moment of Switches Turn-on

In the proposed converter, the equivalent circuit is shown in Fig. 4(a) at the time when the switches are on. For creating ZCS condition, inductors L_1 and L_2 should be discharged, i.e. $i_{L1}(0) = i_{L2}(0) = 0$. With these conditions, the currents i_{L1}, i_{C3} and i_{C1} are obtained. In the impedance source $L_1 = L_2$ and $C_1 = C_2$. As a result, $i_{L1} = i_{L2}$, $V_{L1} = V_{L2}$, $i_{C1} = i_{C2}$ and $V_{C1} = V_{C2}$. The load amount referred to the transformer primary was calculated based on the equivalent circuit of the transformer turns ratio, as follows:

$$R_o' = \left(\frac{N_1}{N_2}\right)^2 .R_0 \qquad (1)$$

The equation is related to the frequency domain. Symbols $V_{C1}(0) = V_{C2}(0)$ and $V_{C3}(0)$ are the capacitors C_1, C_2, C_3 primary voltages. The current values of the capacitors C_1, C_3 and of the inductor L_1 are obtained according to the equations (2), (3). The load is assumed to be resistive.

According to the outlet current equations, for all values of the inductors and capacitors, equations are

www.SID.ir

Archive of SID

[DOI: 10.22068/IJEEE.14.1.49]

Downloaded from ijeee.iust.ac.ir at 11:41 IRDT on Saturday September 5th 2020

stable. Only if the values of the elements C_1, C_2, C_3, C_4, L_1, L_2, L_2, R_o' are equal to zero, equations (2) and (3) are unstable. According to the equation (3), the amounts of C_3 and C_4 are very effective in the currents gain of i_{C3} and i_{C4}. Since i_{C3} and i_{C4} create current stress at the moment of switches turn-on, the capacitors C_3 and C_4 are selected in very small values.

$$i_{C1}(s) = i_{L1}(s) = \frac{C_1C_3R_o'S\left[V_{C1}(t=t_0)-V_{C3}(t=t_0)\right]+C_1V_{C1}(t=t_0)}{C_1C_3L_1R_o'S^3+C_1L_1S^2+R_o'S(2C_1+C_3)+1} \quad (2)$$

$$i_{C3}(s) = -\frac{C_3}{2}\times \left[\frac{C_1L_1V_{C3}(t=t_0)S^2}{C_1C_3L_1R_o'S^3+C_1L_1S^2+R_o'S(2C_1+C_3)+1} + \frac{2C_1R_o'S\left[V_{C3}(t=t_0)-V_{C1}(t=t_0)\right]+V_{C3}(t=t_0)}{C_1C_3L_1R_o'S^3+C_1L_1S^2+R_o'S(2C_1+C_3)+1}\right] \quad (3)$$

The equations (2) and (3) are always stable for the values of the non-zero elements at the moment of switches turn-on where a current shot will not be created. According to the initial value theorem that is expressed in (4), the initial Z-source inductors' currents are zero. As a result, switches S1and S2 turn on under ZCS condition.

$$\lim_{s\to\infty} s\times i_{L1}(s) = 0 \quad (4)$$

In order to achieve the soft switching conditions, the switching frequency of the proposed converter must be lower than the resonant frequency. The equation (5) expresses the occurrence of the ZCS condition.

$$f_s < f_{rzcs} = \frac{1}{2\pi\sqrt{C_1L_1}} \quad (5)$$

The equations (6) and (7) are obtained, if the short circuit occurs in the output i.e. $R_o = 0$. Diode D_1 turns-on at the time of t_2. Practically, there would be a small impedance in the case of the output short-circuit. To rescue of impact function, the amounts of the capacitors C_3 and C_4 are select in very small values,

$$i_{C1}(t_0<t<t_2) = i_{L1}(t_0<t<t_2) = \sqrt{\frac{C_1}{L_1}}V_{C1}(0)\sin\left(\frac{t}{\sqrt{C_1L_1}}\right) \quad (6)$$

$$i_{C3}(t_0<t<t_2) = -\frac{C_3}{2}\left[V_{C3}(0)\delta(t)\right] \quad (7)$$

If the open-circuit condition occurs in the output, the equation (8) is obtains, that is $R_o = \infty$.

$$i_{C1}(t_0<t<t_2) = i_{L1}(t_0<t<t_2) = i_{C3}(t_0<t<t_2) = \sqrt{\frac{C_3}{2L_1}}\left[V_{C1}(0)-V_{C3}(0)\right].\sin\left(\sqrt{\frac{2}{C_3L_1}}t\right) \quad (8)$$

According to Fig. 4(f), at the end of the switching period, the transformer magnetizing current is increasing in the negative direction. The important point is the current value, because at the start of the next cycle, the current will pass through the switches and ZCS will overshadow. As a result, the current value must be reduced for as much as possible. It is depend on choosing the value of the capacitors C_3, C_4.

$$Z_{z_source} = 0.5\left(L_1S+\frac{1}{C_1S}\right) \quad (9)$$

$$Z_{trans+C_3,C_4} = L_mS+\frac{2}{C_3S} \quad (10)$$

$$f_s < f_{rf} = \frac{\sqrt{\frac{1}{2C_1}+\frac{2}{C_3}}}{2\pi\sqrt{L_m+0.5L_1}} \quad (11)$$

According to equations (9) and (10) that eventuate equation (11), in order to magnify $Z_{Trans+C3,C4}$ to charge and discharge, the current of capacitors C_3, C_4 stay small and thus does not affect the ZCS condition. The capacitors C_3, C_4 are selected in very small values. At the end of the switching period, the inductors of the Z-source are fully discharged and the charging current of the capacitors C3and C4 is supplied by Z-source capacitors. According to the restriction of the equation (5), the resonance frequency, in the beginning of the switching period, should be selected slightly larger than the switching frequency to establish minimum peak current of the switches S1and S2. The amounts of the capacitors C_1 and C_2 are always selected larger than the ones of the capacitors C_3 and C_4. As a result, the amount of inductors L_1, L_2 can be selected according to the equations (5) and (11).

$$C_1, C_2 > C_3, C_4 \quad (12)$$

3.2 ZVS at the Moment of Switches Turn-off

Precisely at the moment of switches turn-off, the equivalent circuit will be as shown in Fig. 4(d). At this moment, the capacitors C3and C4 are discharging sharply and the transformer magnetizing current reaches the maximum value after passing through the impedance source. According to Fig. 4(d), the transformer magnetizing current is expressed in equation (13). The equation (13) results the equations (15) and (15). According to equation (15), a resonance is created between Z-source elements and capacitors C_3, C_4 and the transformer magnetizing inductor. The

www.SID.ir

Archive of SID

[DOI: 10.22068/IJEEE.14.1.49]

Downloaded from ijeee.iust.ac.ir at 11:41 IRDT on Saturday September 5th 2020

voltage of the capacitors C_3, C_4 will decrease to zero at the moment of switches-off. As a result, switches will turn off under ZVS condition.

$$i_m(s) = C_3 \frac{A}{S^2 B} \tag{13}$$

where

$$A = A_1 S^3 + A_2 S^2 + A_3 S + A_4$$
$$B = B_1 S^2 + B_2$$
$$A_1 = \left[i_m(t_3) L_m (C_1 L_1 + 1) - L_1 i_{L1}(t_3) \right]$$
$$A_2 = \left[2C_1 L_1 \left(V_{C3}(t_3) - 2V_{C1}(t_3) + V_{in} \right) + 2V_{C3}(t_3) - V_{C1}(t_3) \right]$$
$$A_3 = -\left[L_1 i_{L0}(t_3) \right]$$
$$A_4 = V_{C1}(t_3) - V_{in}$$
$$B_1 = \left[C_1 C_3 L_1 (L_m - L_1) + C_3 L_m \right]$$
$$B_2 = 2C_1 L_1 + C_3 L_1 + 2$$

$$i_m(t_3 < t < t_4) = \left[\frac{A_1 C_3}{B_1} - \frac{A_3 C_3}{B_2} \right] \cos\left(\sqrt{\frac{B_2}{B_1}} t \right) + \left[\frac{A_2 C_3}{\sqrt{B_1 B_2}} - \frac{A_4 \sqrt{B_1} C_3}{B_2 \sqrt{B_2}} \right] \sin\left(\sqrt{\frac{B_2}{B_1}} t \right) + \frac{A_3}{B_1} u(t) + \frac{A_4}{B_2} r(t) \tag{14}$$

$$f_s < f_{rzvs} = \frac{\sqrt{2 + C_3 L_1 + 2C_1 L_1}}{2\pi \sqrt{C_3 L_m (C_1 L_1 + 1)}} = \frac{\sqrt{2}}{2\pi \sqrt{C_3 L_m}} \tag{15}$$

3.3 Possibility to Increase the Working Period to Over 50%

According to Fig. 5, Fig. 4(d), Fig 4(e), as the voltages of the capacitors C_3 and C_4 reach the zero amount, the freewheeling diodes D_2 and D_3 start to conduct the current and transfer the transformer magnetizing inductance current to Z-source. In this case, diode D_1 is conducting the current. In the following, by charging the capacitors C_3 and C_4 by the source impedance, the freewheeling diodes D_2 and D_3 are in reverse bias and capacitors C_1 and C_2 start to charge. Besides, the transformer magnetizing current direction is reversed after the time t_5, according to Fig. (2).

As a result, the transformer magnetizing current increases in the negative direction, i.e. the transformer core resets without the switching period is completed. Therefore, the increasing of the duty cycle to over 50% is possible. At the end of the switching period, transformer magnetizing current is increasing in the negative direction. The important point is the current value because at the beginning of the next cycle, it will pass through the switches S_1 and S_2 and ZCS. As a result, the current value must be reduced as much as possible. It is depend on choosing the values of the capacitors C_1, C_2 and capacitors C_3, C_4 and inductors L_1 and L_2.

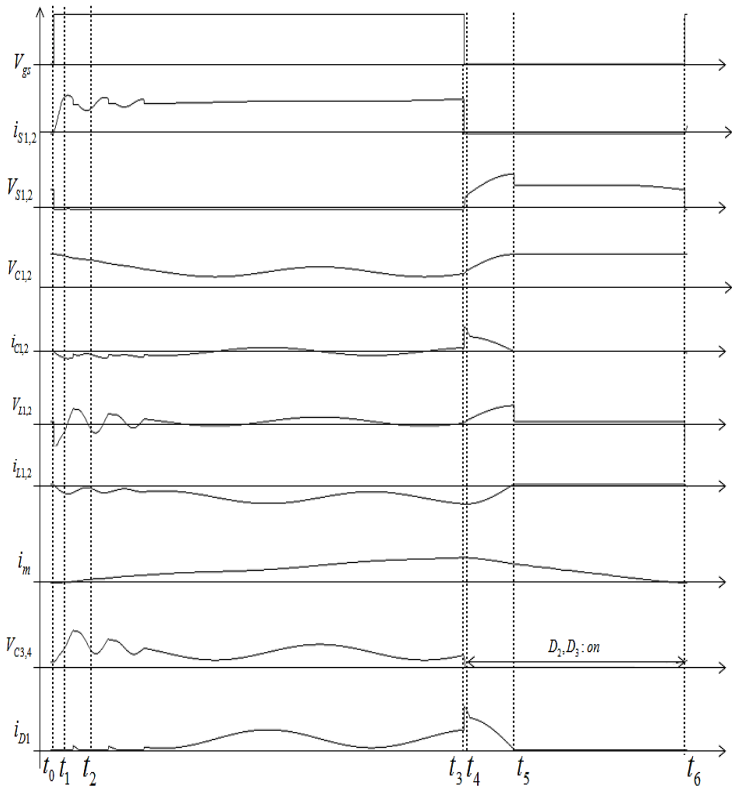


Fig. 5 Waveforms of the proposed converter in the maximum duty cycle.

www.SID.ir

Archive of SID

[DOI: 10.22068/IJEEE.14.1.49]

Downloaded from ijeee.iust.ac.ir at 11:41 IRDT on Saturday September 5th 2020

The maximum duty cycle of efficiency curve occurs when the transformer magnetizing current is zero at the end of the switching period. According to Fig. 5, Freewheeling diodes D_2 and D_3 start to conduct the current and continue conducting until the end of the period after the moment t_4. So Fig. 4(e) is the equivalent circuit until the end of the period. The transformer magnetizing current is obtained by the equation (16) after the moment t_4. The equation (16) is expressed in the frequency domain and the equation (17) is expressed in the time domain.

$$i_m(S) = \frac{2C_1 S\left(L_m i_{Lm}(t=t_5) - L_1 i_L(t=t_5)\right)}{2L_m C_1 S^2 + 1} + \frac{2C_1 V_{C1}(t=t_5)}{2L_m C_1 S^2 + 1} \quad (16)$$

$$i_m(t) = \frac{L_m i_{Lm}(t_5) - L_1 i_L(t_5)}{L_m}\cos\left(\frac{t}{\sqrt{2L_m C_1}}\right) + \frac{V_{C1}(t_5)}{L_m}\sin\left(\frac{t}{\sqrt{2L_m C_1}}\right) \quad (17)$$

The amount of the transformer magnetizing current reaches zero at the moment t_6. The period of the moment t_5 to the moment t_6 makes up almost the two-thirds of being cut of the switches. The maximum duty cycle is expressed in the equation (18).

$$i_m(t=t_6) = 0 \rightarrow D_{\max} = 1 - \left[\frac{3\sqrt{2L_m C_1}}{2T_s}\tan^{-1}\left(\frac{L_1 i_{L1}(t_5) - L_m i_m(t_5)}{V_{C1}(t_5)\sqrt{2L_m C_1}}\right)\right] \quad (18)$$

In order to improve the design, it is important to consider the range of selected z-sources elements. The equations (19), (20) and (21) are derived from the equations (5), (11), (12) and (15).

$$C_3 < \frac{1}{2\pi^2 f_s^2 L_m} \quad (19)$$

$$L_1 < \frac{1}{C_3 \pi^2 f_s^2} - 2L_m \quad (20)$$

$$C_1 < \frac{1}{4\pi^2 f_s^2 L_1} \quad (21)$$

Diode D_1 is turning off at the moment of t_5. The maximum voltage stresses of the switches occur at the moment of t_5. According to the simulation results, the moment of t_5 can approximately be calculated by equation (22). According to equation (23), the voltage of the Switches can be calculated.

$$t_5 = \frac{D + \frac{1}{2}D(1-D)}{f_s} \quad (22)$$

$$V_{s1}\Big|_{(DT_s < t \le t_5)} = V_{s2}\Big|_{(DT_s < t \le t_5)} = \frac{L_m i_{m-\max} - 2L_1 i_{L_{1-\max}}}{\sqrt{L_1 C_1}}\sin\left(\frac{t}{\sqrt{L_1 C_1}}\right) - V_{in} - V_{in}\cos\left(\frac{t}{\sqrt{L_1 C_1}}\right) \quad (23)$$

The voltage gain can be expressed by equation (24) when the duty cycle is in the maximum amount.

$$G = \frac{V_o}{V_{in}} = \frac{1}{2} \times \frac{D_{\max}(1 - D_{\max})}{2D_{\max} - D_{\max}(1 - D_{\max}) - 1} \quad (24)$$

4 Experimental Results

A 2700-watt converter is built according to the values in Table 1. The model has two working modes, first, variable power supply mode and second, welding mode. The output capacitor is removed by a simple relay in the welding mode. As a result the output voltage ripple increases. Increased voltage ripple is very effective in creating a better welding arc. In order to increase the magnetizing inductance of the transformer, the number of the windings is slightly higher when compared with the two-transistor forward converter. In order not to saturate, a too small air gap is mounted on the transformer.

The experimental prototype is built and shown in Fig.6 to verify the correctness of the theories and the effectiveness of the proposed approach. Wave forms practical sample is given in Fig. 7. Selecting the smaller possible capacitors C_3 and C_4 decreases their discharge current but at the moment of shutting down the switches, it affects the ZVS condition. The selection of the capacitors C_3 and C_4 is the best choice as it is shown in Table 1. The duty cycle of the experimental converter is slightly more than 50 percent.

Table 1 The experimental sample values of the design.

Converter Elements	Value
Switches S_1 and S_2	3×2sk4108 (parallel)
Inductors L_1 and L_2	10 µH
Output filter capacitor	3300 µf
Output filter inductor	30 µH
Capacitors $C_1$and C_2	100 nf
Capacitors $C_3$and C_4	3.3 nf
Diodes D_1	DSEI30-12
Diodes D_4 and D_5	5×D9202 (parallel)
Operation frequency	50 kHz
Input voltage	280–310 V_{DC}
Output voltage Mode 1 (Variable power supply) Mode 2 (Welding)	12–30V_{DC}/65V_{DC} (OC)
Output current	Up to 100 A
Transformer turn ratio	10:3
Diodes D_2 and D_3	MUR15120
Transformer magnetizing inductance	1.05 mH

www.SID.ir

Archive of SID

[DOI: 10.22068/IJEEE.14.1.49]

Downloaded from ijeee.iust.ac.ir at 11:41 IRDT on Saturday September 5th 2020

Fig. 10 shows the proposed converter control method. The control method is cycle by cycle. In this way, the transistors gate pulses are depend on the output load. The current and voltage feedback are harmoniously together and the final drive pulse is created from comparing the two voltages and currents feedback. The output voltage and the output current are adjusted by two potentiometers by the user. Fig. 11 shows the gate source waveforms in different conditions and the cycle by cycle control method is visible.

5 Conclusion

This paper presents a new topology named novel two transistors forward topology employing a z-source to achieve ZVZCS and power transformer resetting with ability to increase the duty cycle to over 50%. A practical 2700 watt and 12-30 volt sample of the proposed model was constructed. The proposed model, can supply a current up to 100A for welding applications. The switching losses have decreased to a great extent at the moments of the switching. The efficiency of the proposed converter exceeds 94.5% in a full load. The efficiency can reach the maximum of 96%. With regarding the characteristics of the proposed converter, this converter is suitable for multifunction applications with high efficiency such as welding, charging types of batteries etc.

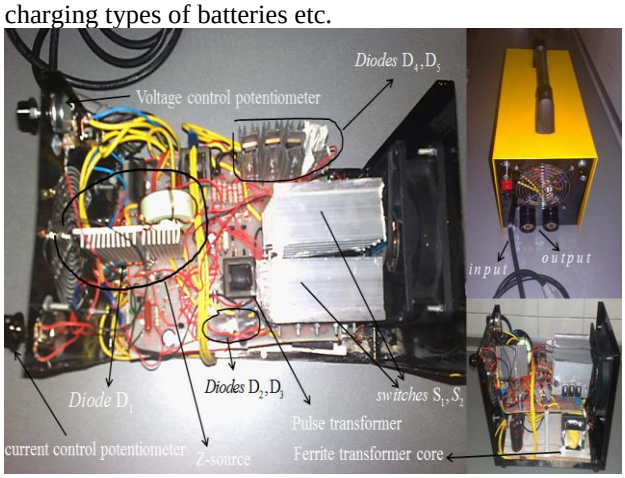


Fig. 6 The prototype of the proposed converter.

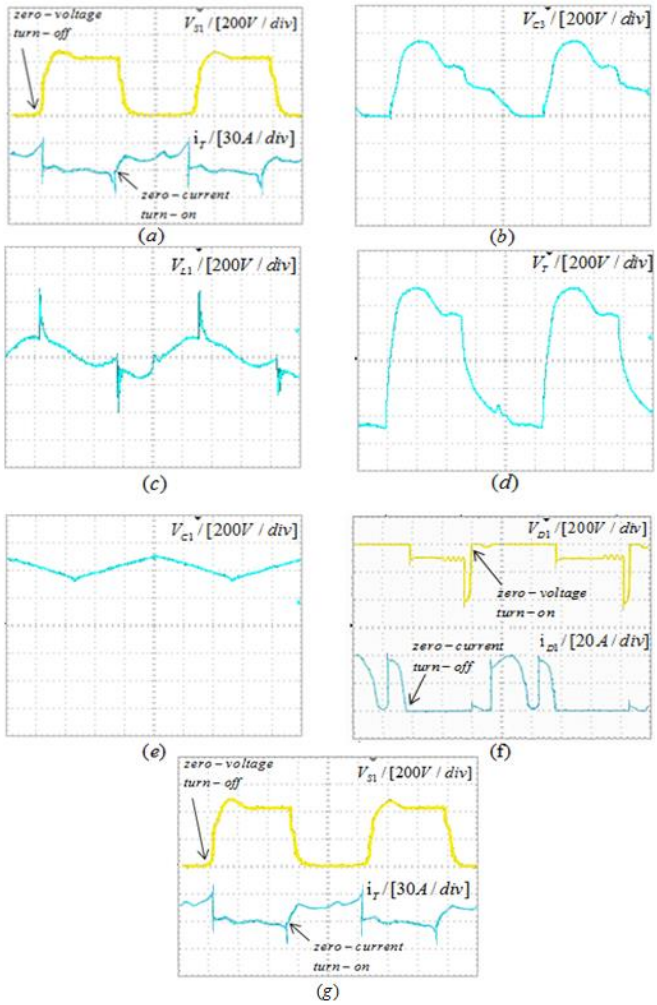


Fig. 7 Experimental waveforms: a) ZVS and ZCS of S_1, S_2 (V_{in} = 310 VDC, I_o = 90 A, V_o = 30 VDC), b) V_{C3} (V_{in} = 310 VDC, I_o = 90 A, V_o = 30 VDC), c) V_{L1} (V_{in} = 310 VDC, I_o = 90 A, V_o = 30 VDC), d) V_T (V_{in} = 310 VDC, I_o = 90 A, V_o = 30 VDC), e) V_{C1} (V_{in} = 310 VDC, I_o = 90 A, V_o = 30 VDC), f) ZVS and ZCS of D_1 (V_{in} = 310 VDC, I_o = 90 A, V_o = 30 VDC), g) ZVS and ZCS of S_1, S_2 in welding mode (V_{in} = 310 VDC, I_o = 100 A, V_o = 28 VDC).

www.SID.ir

Archive of SID

[DOI: 10.22068/IJEEE.14.1.49]

Downloaded from ijeee.iust.ac.ir at 11:41 IRDT on Saturday September 5th 2020

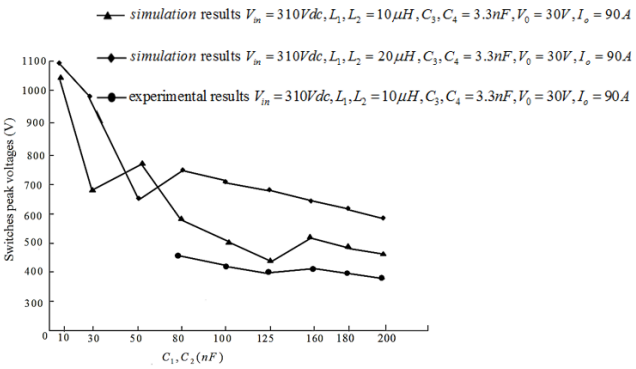


Fig. 8 The proposed conversion peak voltage stress.

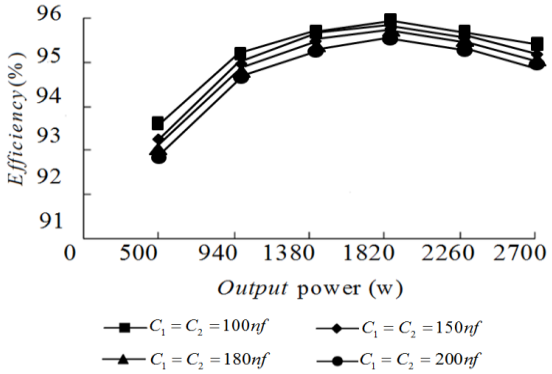


Fig. 9 The proposed conversion efficiency curve.

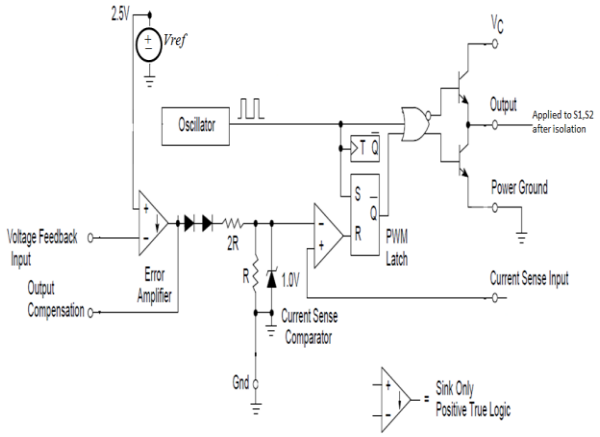


Fig. 10 Cycle by cycle control method.

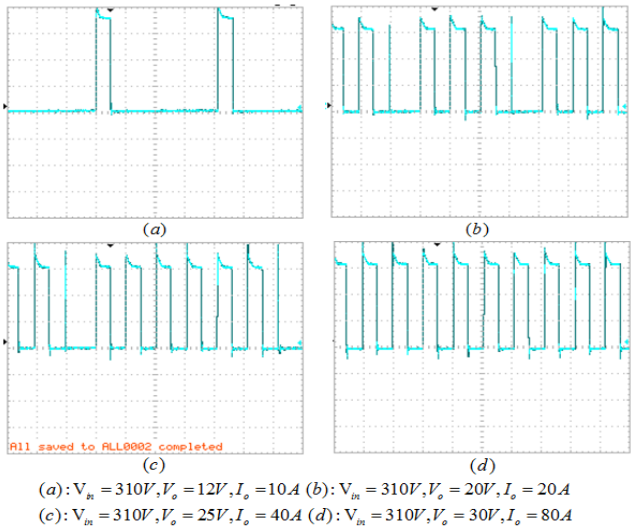


Fig. 11 Gate source waveforms (cycle by cycle control method).

References

[1] H. Wu, and Y. Xing, "Families of Forward converters Suitable for Wide Input Voltage Range Applications," *IEEE Transactions on Power Electronics*, Vol. 29, No. 11, pp. 6006–6017, 2014.

[2] B. R. Lin, H. K. Chiang, C. C. Chen, C. S. Lin, and A. Chiang, "Analysis and implementation of soft switching converter with series-connected transformers," *IET Electric Power Applications*, Vol. 1, No. 1, pp. 82–92, 2007.

[3] N. Murakami, and M. Yamasaki, "Analysis of a resonant reset condition for a single-ended forward converter," in *19th Annual IEEE Power Electronics Specialists Conference*, Kyoto, Japan, pp. 1018–1023, 1998.

[4] X. Xie, J. Zhang, and G. Luo, "An improved self-driven synchronous rectification for a resonant reset forward," in *18th Annual IEEE Applied Power Electronics Conference and Exposition*, Miami Beach, FL, USA, pp. 348–351, 2003.

[5] G. Spiazzi, "A high-quality rectifier based on the forward topology with secondary-side resonant reset," *IEEE Transactions on Power Electronics*, Vol. 18, No. 3, pp. 725–732, 2003.

[6] J. A. Cobos, O. Garcia, J. Sebastian, and J. Uceda, "Resonant reset forward topologies for low output voltage on-board converters," in *Ninth Annual Applied Power Electronics Conference and Exposition*, Orlando, FL, pp. 703–708, 1994.

[7] F. D. Tan, "The forward converter: from the classic to the contemporary," in *17th Annual IEEE Applied Power Electronics Conference and Exposition*, Dallas, TX, pp. 40–47, 2002.

[8] J. A. Cobos, O. Garcia, and J. Uceda "Comparison of high efficiency low output voltage forward topologies," in *25th Annual IEEE Power Electronics Specialists Conference*, Taipei, pp. 887–894, 1994.

[9] Y. Xi, and P. Jain, "A forward converter topology employing a resonant auxiliary circuit to achieve soft switching and power transformer resetting," *IEEE Transactions on Industrial Electronics*, Vol. 50, No. 1, pp. 132–140, 2003.

[10] L. Petersen, "Advantages of using a two-switch forward in single-stage power factor corrected power supplies," in *22nd International Telecommunications Energy Conference*, Phoenix, AZ, pp. 325-331, 2000.

www.SID.ir

Archive of SID

[DOI: 10.22068/IJEEE.14.1.49]

Downloaded from ijeee.iust.ac.ir at 11:41 IRDT on Saturday September 5th 2020

[11] X. Ruan, B. Li, and Q. Chen, "Three-level converters- a new approach for high voltage and high power DC-to-DC converter," in *33rd Annual Power Electronics Specialists Conference Cairns*, Qld., Australia, pp. 663–668, 2002.

[12] Y. Gu, and Z. Lu, "A Novel ZVS Resonant Reset Dual Switch Forward DC–DC Converter," *IEEE Transactions on Power Electronics*, Vol. 22, No. 1, pp. 96–102, 2007.

[13] E. Adib, and H. Farzanehfard, "Analysis and Design of a Zero-Current Switching Forward Converter with Simple Auxiliary Circuit," *IEEE Transactions on Power Electronics*, Vol. 27, No. 1, pp. 144–150, 2012.

[14] F. Z. Peng, "Z-source inverter," *IEEE Transactions on Industry Applications*, Vol. 39, No. 2, pp. 504–510, 2003.

[15] B. Poorali, A. Torkan, and E. Adib, "High step-up Z-source DC-DC converter with coupled inductors and switched capacitor cell," *IET Power Electronics*, Vol. 8, No. 8, pp. 1394–1402, 2015.

[16] B. M. Ge, Q. Lei, W. Qian, and F. Z. Peang, "A family of Z-source matrix converters," *IEEE Transactions on Industrial Electronics*, Vol. 59, No. 1, pp. 35–46, 2012.

[17] M. S. Shen, J. Wang, A. Joseph, F. Z. Peng, L. M. Tolbert, and A. J. Adams, "Constant boost control of the Z-source inverter to minimize current ripple and voltage stress," *IEEE Transactions on Industry Applications*, Vol. 42, No. 3, pp. 770–778, 2006.

[18] M. Poursmaeil, S. M. Dizgah, H. Torkaman, and E. Afjei, "Autonomous Control and Operation of an Interconnected AC/DC Microgrid with Γ-Z-Source Interlinking Converter," in *Smart Grids Conference (SGC)*, Tehran, Iran, 2017.

[19] M. Poursmaeil, S. M. Dizgah, H. Torkaman, and E. Afjei, "Small signal modeling, analysis and control of Γ-Z-Source Inverter," in *Iranian Conference on Electrical Engineering (ICEE)*, Tehran, Iran, pp. 1216–1222, 2017.

[20] M. S. Shen, A. Joseph, J. Wang, F. Z. Peng, and A. D. J. Adams, "Comparison of traditional inverters and Z-source inverter for fuel cell vehicles," *IEEE Transactions on Power Electronics*, Vol. 22, No. 4, pp. 1453–1463, 2007.

[21] H. Torkaman, N. Karami, and M. M. Nezamabadi, "Design, Simulation, Validation and Comparison of New High Step-up Soft Switched Converter for Fuel Cell Energy System," *Journal of Energy Management and Technology*, Vol. 1, No. 1, pp. 53–60, 2017.

[22] M. Einan, H. Torkaman, and M. Pourgholi, "Optimized Fuzzy-Cuckoo Controller for Active Power Control of Battery Energy Storage System, Photovoltaic, Fuel Cell and Wind Turbine in an Isolated Micro-Grid," *Batteries*, Vol. 3, No. 23, pp. 1–18, 2017.

[23] F. Z. Peng, A. Joseph, J. Wang, M. Shen, L. H. Chen, Z. G. Pan, E. Ortiz-Rivera, and Y. Huang, "Z-source inverter for motor drives," *IEEE Transactions on Power Electronics*, Vol. 20, No. 4, pp. 857–863, 2005.

[24] D. Vinnikov, and A. I. Roasto, "Quasi-Z-source-based isolated DC/DC converters for distributed power generation," *IEEE Transactions on Industrial Electronics*, Vol. 58, No. 1, pp. 192–201, 2011.

[25] H. Khaligh, H. Torkaman, and A. Ebrahimian, "Novel Algorithm for Optimum Output Passive Filter Design in 400 Hz Inverter," in *9th Annual International Power Electronics, Drive System, and Technologies Conference*, Tehran, Iran, 2018.

[26] S. Khosrogorji, M. Ahmadian, H. Torkaman, and S. Soori, "Multi-input DC/DC converters in connection with distributed generation units – A review," *Renewable and Sustainable Energy Reviews*, Vol. 66, pp. 360–379, 2016.

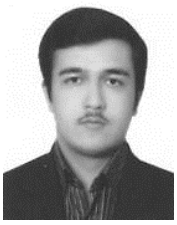
[27] S. Khosrogorji, H. Torkaman, and F. Karimi, "A short review on multi-input DC/DC converters topologies," in *The 6th Power Electronics, Drive Systems & Technologies Conference (PEDSTC)*, Tehran, Iran, pp. 650-654, 2015.

[28] Z. Yan, L. Liming, and L. Hui, "A High-Performance Photovoltaic Module-Integrated Converter (MIC) Based on Cascaded Quasi-Z-Source Inverters (qZSI) Using eGaN FETs," *IEEE Transactions on Power Electronics*, Vol. 28, No. 6, pp. 2727–2738, 2013.

[29] F. Z. Peng, M. S. Shen, and K. Holland, "Application of Z-source inverter for traction drive of fuel cell-battery hybrid electric vehicles," *IEEE Transactions on Power Electronics*, Vol. 22, No. 3, pp. 1054–1061, 2007.



H. Torkaman received the Ph.D. degree in in Electrical Engineering, Tehran, Iran, 2011. He is currently an Associate Professor at the Faculty of Electrical Engineering, Shahid Beheshti University, Tehran, Iran. His main research interests include electrical machines, power electronics and renewable energies.



T. Hemmati received the B.Sc. and M.Sc. degrees from the Zanjan University and Shahid Beheshti University, Tehran, Iran, in 2013 and 2015 respectively. His research interests include power electronic and switching power supply.

www.SID.ir